Small molecule-mediated insulin hypersecretion induces transient unfolded protein response and loss of function in pancreatic islet beta cells

Short title: Chronic stimulation of beta cells induces a transient ER stress response

Karina Rodrigues-dos-Santos[1†], Gitanjali Roy[1†], Derk D. Binns[2†], Magdalena G. Grzemska[2], Luiz F. Barella[1], Fiona Armoo[1], Melissa K. McCoy[3], Andrew V. Huynh[2], Jonathan Z. Yang[2], Bruce A. Posner[3], Melanie H. Cobb[2], and Michael A. Kalwat[1,4,] *

[1]Lilly Diabetes Center of Excellence, Indiana Biosciences Research Institute, Indianapolis, IN, USA;

Departments of [2]Pharmacology and [3]Biochemistry, UT Southwestern Medical Center, Dallas, TX, USA;

[4]Center for Diabetes and Metabolic Diseases, Indiana University School of Medicine, Indianapolis, IN, USA.

[†]Authors contributed equally

ORCID identifiers: MAK, 0000-0002-8349-9470; MHC, 0000-0003-0833-5473

*Correspondence: mkalwat@indianabiosciences.org or mkalwat@iu.edu

Word count: 4389

ABSTRACT:

Aims/hypothesis Insulin production and its regulated exocytosis by pancreatic islet beta cells is the major physiological mechanism controlling blood glucose concentrations. Beta cells are susceptible to failure due to genetic and environmental influences, leading to type 1 and 2 diabetes. In this work we aimed to advance understanding of the regulation of beta-cell function by identifying small molecule modulators of secretion.

Methods For high-throughput screening and routine medium-throughput beta cell function assays we used mouse MIN6 beta cells stably expressing a Gaussia luciferase-linked insulin secretion reporter (InsGLuc-MIN6). We validated hit small molecules using cadaveric human islets in static culture insulin secretion assays. We measured effects on calcium influx and cAMP in MIN6 cells using Fura-2 and a bioluminescence resonance energy transfer reporter assay, respectively. Metabolism was analyzed by

targeted metabolomics and Seahorse oxygen consumption assays. We measured relative gene expression and protein amounts by quantitative RT-PCR and SDS-PAGE immunoblotting, respectively.

Results Through our high-throughput screen we discovered 2-(3-benzyl-2-iminobenzimidazol-1-yl)-1-thiophen-2-ylethanol (SW016789) which acutely potentiated nutrient-induced calcium influx and insulin secretion. More than 2 hours of exposure to SW016789 transiently induced the unfolded protein response of the endoplasmic reticulum and shut down of insulin secretory function. Distinct from the effects of thapsigargin, SW016789 did not affect beta cell viability or death as determined by multiplexed cytotoxicity assays and a lack of induction of cleaved PARP. This may be due in part to a more rapid induction of *Hspa5*, and a lesser induction of signalling through the eIF2α kinase PERK and lack of expression of oxidative stress genes like *Txnip*. We determined that SW016789 acted upstream of the voltage-dependent calcium channel (VDCC) and potentiated nutrient-stimulated, but not KCl-stimulated, calcium influx. The potentiating effects of SW016789 were not due to altered metabolic pathways, mitochondrial function, or actions on G protein-coupled receptors. In chemical co-treatment experiments we discovered synergy between SW016789 and small molecule activators of protein kinase C and VDCCs, suggesting potential involvement of these pathways in the mechanism of action. Finally, chronically elevated calcium influx was required for the inhibitory impact of SW016789, as co-treatment with dihydropyridine-class VDCC inhibitors protected MIN6 beta cells and human islets from loss of function.

Conclusions/interpretation These data suggest the major mechanism of action of SW016789 in beta cells is to potentiate opening of VDCCs. This activity may partially depend on protein kinase C. Beta cells under pharmacological hypersecretory conditions have the capacity to suppress their function to mitigate ER stress and avoid apoptosis. Further study of the mechanisms underlying these processes will increase understanding of beta cell function in normal and pathophysiological states.

Research in context

What is already known about this subject?

- Pharmacologic and environmental chemicals can stimulate aberrant beta cell activity.
- Hypersecretion of insulin from pancreatic beta cells can cause ER stress and lead to beta cell dysfunction.
- Defects in beta cell ER stress handling contribute to diabetes pathogenesis.

What is the key question?

- Can the chemical tool SW016789 help uncover novel insulin secretion regulatory pathways and ER proteostasis factors?

What are the new findings?

- SW016789 caused hypersecretion of insulin via enhanced nutrient-stimulated Ca^{2+} influx followed by transient ER stress and shutdown of beta cell function without apoptosis.
- Blockade of voltage-dependent Ca^{2+} channels protected human islets and beta cells from hypersecretion-induced dysfunction.

How might this impact on clinical practice in the foreseeable future?

- These results have the potential to uncover beta cell ER stress mitigation factors and add support to beta cell rest strategies to preserve function.

INTRODUCTION

Pancreatic islet beta cells sense and control circulating glucose concentrations by secreting insulin. In type 1 diabetes (T1D), autoimmune attack on beta cells results in their death and thus a lack of insulin. In type 2 diabetes (T2D), beta cells initially compensate for insulin resistance but eventually fail to secrete sufficient insulin to maintain euglycemia [1]. Interventions are aimed at restoring beta cell functionality, lowering insulin resistance, and reducing hyperglycaemia. However, existing therapeutics have limitations, necessitating identification of new targets and pathways.

Beta cells sense elevated circulating blood glucose concentrations via the glucose transporters GLUT1/3 [2]. Upon cellular entry, glucose metabolism via glycolysis and the tricarboxylic acid cycle yields a relative increase in [ATP/ADP], causing ATP-sensitive potassium (K_{ATP}) channel closure. This closure reduces the plasma membrane permeability to potassium, causing membrane depolarization, opening of voltage-dependent Ca^{2+} channels (VDCCs) and Ca^{2+} influx [3]. Ca^{2+} influx also stimulates oxidative phosphorylation in the mitochondria, driving a metabolic cycle that sustains ATP production and insulin secretion [4, 5]. Ca^{2+} influx triggers the fusion of insulin secretory vesicles with the plasma membrane resulting in insulin exocytosis [6]. Nutrient metabolism further enhances secretion without further Ca^{2+} influx via the amplifying pathway [7-9]. To handle their specialized secretory function, beta cells engage the unfolded protein response of the endoplasmic reticulum (UPR^{ER}) [10]. The UPR^{ER} is crucial in beta cells, as its disruption (e.g., PERK loss-of-function) leads to beta cell failure and diabetes [11]. Conversely, unmitigated UPR^{ER} is also detrimental to beta cell function and survival, eventually leading to induction of pro-apoptotic transcription factors including *Ddit3* (CHOP) and *Txnip* [12, 13].

Many studies have elucidated aspects of beta cell biology that may be targeted to improve overall beta cell health and function, including the UPR^{ER}, beta cell dedifferentiation, and the role of immature beta cells in whole islet function [14-18]. However, the high-throughput identification of novel small molecules that alter pancreatic beta cell function has lagged in comparison. Here, we used a secreted insulin-luciferase-based high-throughput screening tool to identify a small molecule, SW016789, which acutely and chronically alters beta cell secretory responses [19, 20]. We hypothesised the chronic effects on function were a result of acute hypersecretion which induced stress pathways (e.g., ER stress) that led to a shutdown of beta cell function, but not beta cell death. We investigated the mechanisms of action of SW016789 using a multipronged approach including measuring Ca^{2+} influx, cAMP generation, and insulin secretion; metabolomics and mitochondrial function; gene expression; and co-treatment with compounds that may interfere with the effects of SW016789. Our results with SW016789 agree with a model of beta cell plasticity wherein the effects of persistent secretory stress are mitigated to avoid cell death at the expense of function. Chemical tools like SW016789 present an opportunity to discover previously unrecognized or poorly characterized genes and pathways involved in these processes in the beta cell.

METHODS:

Antibodies and Reagents – Source information for all small molecules and antibodies used in this work are listed in electronic supplementary material (ESM) **Table S4**.

Cell culture and treatments – MIN6 beta cell culture has been described [20]. Prior to glucose stimulation experiments, cells were washed twice with and incubated for 2 h in freshly prepared glucose-free modified Krebs-Ringer bicarbonate (KRBH) buffer (5 mM KCl, 120 mM NaCl, 15 mM HEPES, pH 7.4, 24 mM $NaHCO_3$, 1 mM $MgCl_2$, 2 mM $CaCl_2$, and 1 mg/ml radioimmunoassay-grade BSA). Cells were lysed in 1% NP40 lysis buffer (25 mM HEPES, pH 7.4, 1% Nonidet P-40, 10% glycerol, 137 mM NaCl, 1 mM EDTA, 1 mM EGTA, 50 mM sodium fluoride, 10 mM sodium pyrophosphate, 1 mM sodium orthovanadate, 1 mM phenylmethylsulfonyl fluoride, 10 µg/ml aprotinin, 1 µg/ml pepstatin, 5 µg/ml leupeptin), rotated (10 min, 4°C), centrifuged (10,000 x g; 10 min; 4°C), and stored at -80°C. MIN6 cells were stimulated with glucose as indicated and secreted insulin and insulin content were measured using HTRF assays (Cisbio). InsGLuc-MIN6 cells were generated and characterized as previously described [20] and were determined to be negative for mycoplasma Detailed description of secreted Gaussia assays and high-throughput screening of small molecules in InsGLuc-MIN6 cells has been described in detail [21] and is expanded in the **ESM Methods**.

Human islet culture – Human islets were cultured upon receipt in complete CMRL-1066 (10% FBS, 100 U/ml penicillin, 100 µg/ml streptomycin). Isolation details included in **ESM Methods**. In static culture insulin secretion experiments, islets were picked under a dissection microscope and transferred to low-binding 1.5 ml tubes (50 islets/tube). Islets were washed twice with KRBH (134 mM NaCl, 4.8 mM KCl, 1 mM $CaCl_2$, 1.2 mM $MgSO_4$, 1.2 mM KH_2PO_4, 5 mM $NaHCO_3$, 10 mM HEPES pH 7.4, 0.1% radioimmunoassay-grade BSA) and preincubated in KRBH (1 mM glucose; 1 h) before switching to buffer containing either 1 or 16 mM glucose for 1 h. Supernatants were collected, centrifuged (10,000 x g; 5 min) and transferred to fresh tubes for storage at -80°C. Total insulin content was extracted by acid-ethanol (1.5% HCl in 70% ethanol) overnight at -80°C and the solution was neutralized with an equal volume of 1 M Tris pH 7.4 prior to insulin assays. Secreted insulin and insulin content were measured using HTRF assays. Human islet characteristics and donor information are listed in **ESM Human Islet Checklist**.

Ca^{2+} and cAMP reporter assays – Ca^{2+} influx measurements were completed in MIN6 cells plated in triplicate in black-walled clear-bottom 96-well tissue culture imaging plates. Cells were preincubated for 1 h in glucose-free KRBH, followed by loading with Fura-2-LR-AM (5 µM) for 25 min and a 5 min washout. Using a BioTek Synergy H1 plate reader equipped with dual monochromators, relative Ca^{2+} levels were measured ($Ex_{340/380}/Em_{510}$ gain=150). Recordings included 5 min baseline followed by 5-30 min post-addition of stimulation as indicated. For relative cAMP measurements, the genetically-encoded Epac-based bioluminescence-resonance energy transfer (BRET) reporter for cAMP (CAMYEL) was used as previously described [22]. CAMYEL MIN6 cells were preincubated in glucose-free KRBH for 1.5 h. Cells were incubated for 15 min at room temperature with coelenterazine-h (20 µM). After a 3 min baseline recording, stimulations were added, and plate read for an additional 15 min. Emission signals at 485/20 and 528/20 nm (center/bandpass) were measured every 0.8 s. Data were normalized by subtracting the mean of the respective baseline reads. Area under the curves (AUCs) were calculated in GraphPad Prism using a baseline of 0 ΔRFU and ignoring peaks that are <10% of the distance from minimum to maximum ΔRFU and those defined by fewer than 15 adjacent points. All peaks must go above the baseline.

Immunoblotting – 40-50 µg of cleared cell lysates were separated on 10% gels by SDS-PAGE and transferred to nitrocellulose for immunoblotting. All membranes were blocked in Odyssey blocking buffer (Licor) for 1 h before overnight incubation with primary antibodies diluted in blocking buffer. After three 10 min washes in TBS-T (20 mM Tris-HCl pH 7.6, 150 mM NaCl, 0.1% Tween-20), membranes

were incubated with fluorescent secondary antibodies for 1 h at room temperature. After three 10 min washes in TBS-T, membranes were imaged on a Licor Odyssey scanner.

Gene Expression – RNA was isolated from MIN6 cells using the PureLink RNA Mini Kit (Life Technologies) or the Aurum Total RNA Mini kit (Bio-Rad). Briefly, after indicated treatments, medium was removed from cells and lysis buffer (with β-mercaptoethanol) was added to cells. Cells were scraped, lysates transferred to 1.5 mL tubes on ice and then transferred to -80°C for storage. Samples were processed according to the kit manufacturer's instructions, including on-column digestion with RNase-free DNase. RNA concentration was measured using an Implen Nanophotometer or Nanodrop spectrophotometer and verified to have $A_{260/280}$ ratios >2.0. 1000 ng of RNA was converted into cDNA using the iScript cDNA synthesis kit (Bio-Rad) following manufacturer instructions and the resulting cDNA was diluted 20-fold with water. One µl of diluted cDNA was used in 10 µl qPCR reactions using 2X SYBR Bio-Rad master mix and 250 nM of each primer. Reactions were run in 384-well format on a CFX384 (Bio-Rad) or QuantStudio 5 (Thermo). qPCR data was analyzed using CFX Manager (Bio-Rad) with 18S RNA as the reference gene. Relative expression was calculated by the $2^{-\Delta\Delta Ct}$ method. All primer details are listed in ESM **Table 4.**

Bioenergetics and Metabolomics – ESM Methods contains detailed descriptions of Seahorse assays, sample preparation, and LC/MS/MS metabolomics analyses.

Statistical Analysis – Quantitated data are expressed as mean ± SD. Data were evaluated using one- or two-way ANOVA as indicated and considered significant if $P < 0.05$. Graphs were made in GraphPad Prism 9 and figures assembled in Affinity Designer (Serif).

RESULTS

High-throughput screen identifies small molecule modulator of insulin secretion.

To discover modulators of beta cell function, we performed a small molecule screen using InsGLuc-MIN6 beta cells [20] (**Fig. 1a**). Our approach involved treating cells with compound for 24 h prior to the assay to probe a distinct phenotypic space, complementary to acute treatments [19]. One of the hits SW016789 inhibited secretion in InsGLuc-MIN6 cells with an IC_{50} <1 µM (**Fig. 1b**) and was chosen for further study. Glucose-stimulated InsGLuc secretion was blunted in MIN6 cells exposed to SW016789 for 24 h, validating screening results (**Fig. 1c**). Chronic treatment of isolated human islets with SW016789 also impaired glucose-stimulated insulin secretion (GSIS) (**Fig. 1d**). SW016789 was

not cytotoxic in MIN6 cells treated for up to 72 h (**Fig. 1e**). During this time course, SW016789-treated cells remained unresponsive to stimulation with glucose or KCl (**Fig. 1f**), but were able to mount significant, although blunted, responses to glucose if combined with stimulators of cAMP generation or protein kinase C (PKC) activation (**Fig. 1f**). Beta cells exposed to SW016789 for 24 h recovered function after a 48 h washout (**Fig. 1g**), indicating the effects are reversible.

SW016789 acutely potentiates nutrient-stimulated insulin secretion

We determined that exposure of InsGLuc-MIN6 cells to SW016789 for 4-8 h resulted in significant inhibition of GSIS while acute (≤2 h) exposure caused a marked potentiation of GSIS (EC_{50} = 2.7 μM) (**Fig. 2a, ESM Fig. 1a,b**). Structure-activity relationship studies revealed that while SW016789 is chiral, both enantiomers retain activity (**ESM Fig. 1c-f**) and the alcohol at the chiral center is important for activity (**ESM Fig. 1g**). SW016789 potentiated amino acid-induced secretion (**Fig. 2b**) but had no effect in cells treated with diazoxide and depolarizing KCl (**Fig. 2c**). However, SW016789 elicited a response from cells treated with diazoxide and glucose without elevated KCl. These data suggested the pathway activated by SW016789 requires nutrient metabolism and may impact Ca^{2+} influx.

Accordingly, chronic SW016789 treatment suppressed glucose-stimulated Ca^{2+} influx (GSCa) (**Fig. 3a,b**), and acute SW016789 treatment potentiated nutrient- but not KCl-stimulated Ca^{2+} influx (**Fig. 3c-f**). Considering these results, we determined the effects of SW016789 on Ca^{2+} influx in the diazoxide paradigm. Beta cells were either pre-treated for 24 h or treated with compound simultaneously with stimulation. With chronic SW016789, stimulation with depolarizing KCl or KCl/glucose caused a rapid and sustained rise in Ca^{2+} influx which was significantly lower than control by ~40% (**ESM Fig. 2a**), while acute SW016789 had no impact (**ESM Fig. 2b**). We also observed a slight increase in GSCa even in the presence of diazoxide and low KCl (**ESM Fig. 2c**), which was consistent with the secretion data (**Fig. 2C**).

A potential source of the SW016789-enhanced Ca^{2+} influx is the endoplasmic reticulum (ER). We tested whether SW016789 impacted ER Ca^{2+} stores or store-operated Ca^{2+} entry (SOCE). MIN6 beta cells were pre-treated with SW016789 for 24, 6, and 2 h and subjected to Ca^{2+} assays including thapsigargin stimulation to block SERCA2, leading to an observable Ca^{2+} leak into the cytosol (**ESM Fig. 2d**). Treatment with SW016789 did not alter this indirect measure of ER Ca^{2+}. Subsequently, Ca^{2+} was reintroduced to measure SOCE. Pre-exposure to SW016789 for 2-6 h caused a small, but significant, decrease in SOCE, but this effect was absent in cells treated for 24 h, suggesting that in beta cells exposed to SW016789, ER Ca^{2+} and SOCE responses were largely unmodified and may not

underlie the acute potentiating or chronic inhibitory effects of SW016789. Additionally, SW016789 did not impact muscarinic receptor-linked Gαq-stimulated Ca^{2+} influx (**ESM Fig. 2e**).

Acute potentiating activity is commonly associated with activation of Gαs-linked G protein-coupled receptors (GPCRs) and may underlie SW016789 actions. To monitor relative cAMP production we used the BRET reporter CAMYEL stably expressed in MIN6 cells [22]. We found that SW016789 or glucose alone each had no effect, while the positive control (forskolin+IBMX) caused a marked increase in cAMP (**Fig. 3g,h**). Notably, SW016789 in the presence of glucose caused a slight but significant increase in signal; however, the response was delayed by about 10-15 min compared to the positive control.

Because of the cAMP and Ca^{2+} results, we considered SW016789 may act through a GPCR. We submitted SW016789 for screening against the GPCR library at the NIMH Psychoactive Drug Screening Program at University of North Carolina [23] (**ESM Fig. 3a**). Overall, SW016789 exhibited little activity across much of the GPCR panel and lacked marked effects on well-known GPCRs in the beta cell (**ESM Table 1**). Only CXCR7 out of 320 GPCRs was a substantial primary hit and confirmation studies determined the EC_{50} of SW016789 on CXCR7 was ~26 μM (**ESM Fig. 3b**). Additionally, the CXCR7 agonist VUF11207 had little impact on InsGLuc secretion during chronic or acute treatments (**ESM Table 2**). These data suggested CXCR7 is unlikely to mediate the effects of SW016789 in beta cells where its activity is observed in the 1-5 μM range.

Beta cell metabolomic and mitochondrial responses are normal following acute SW016789 exposure

Because SW016789 required nutrient co-stimulation to elicit effects on Ca^{2+} influx, we hypothesised altered metabolism may contribute to the mechanism of action. To test this, we performed targeted metabolomics on MIN6 beta cells stimulated with or without glucose in the presence of DMSO or SW016789 for 30 min (**Fig. 4a**). The amplifying effect of SW016789 on GSIS was confirmed and the cellular extracts were submitted for metabolomic analysis (**Fig. 4b, ESM Table 3**). Expectedly, glucose induced glycolysis and TCA intermediates, as well as the reduced/oxidized glutathione ratio (**Fig. 4c,d**). In each of these cases, SW016789 had no impact. These results suggested SW016789 is unlikely to exert effects by acutely altering well-known metabolic pathways. Mitochondrial function was also unaffected by acute exposure to SW016789 (**Fig. 4e-g**).

Chronic amplification of secretion leads to transient UPR^{ER} and shutdown of beta cell function

Acute SW016789-induced insulin hypersecretion eventually caused beta cells to lose normal GSCa and GSIS responses which we hypothesised was due to the UPR^{ER}. To test this, we treated MIN6 cells in a time-course with SW016789 or thapsigargin and collected RNA and protein for analysis (**Fig. 5a**). Acute SW016789 increased immediate early gene (IEG) expression within 1 h which decreased to near baseline by 2-6 h (**Fig. 5b**), in agreement with observed GSCa effects. Thapsigargin had little impact on IEGs. SW016789 also induced expression of UPR^{ER} genes by ~1 h with a peak from 2-6 h depending on the specific gene (**Fig. 5c**), followed by a return to near baseline by 24 h. This was in stark contrast to thapsigargin which caused a similar fold induction, but delayed peak of UPR^{ER} gene expression which persisted at 24 h. Notably, the oxidative stress transcription factor *Txnip* was induced only by thapsigargin. Over the time-course, SW016789 did not significantly alter insulin gene expression, but thapsigargin caused a decrease after 24 h (**Fig. 5d**). SW016789 decreased insulin protein content at 6 h but caused no further decrease by 24 h (**Fig. 5e**), suggesting the effect was due to the induced hypersecretion and implied that after shutdown of beta cell function the drop in insulin content halted. We observed a similar pattern of induction and return to baseline of UPR^{ER} genes with higher doses of SW016789 (**Fig. 6**), indicating SW016789 did not induce terminal UPR^{ER} as occurs with thapsigargin. We also tested other endocrine cells that express stimulus-secretion coupling machinery similar to beta cells, including a human delta cell line and a mouse intestinal L cell line. SW016789 had minimal effects on IEGs or UPR^{ER} genes in these lines, while thapsigargin robustly induced the UPR^{ER} (**ESM Fig. 4**).

In agreement with gene expression data, we observed differences at the protein level between SW016789 and thapsigargin for UPR^{ER} and apoptotic components (**Fig. 7a**). Thapsigargin, but not SW016789, significantly induced CHOP and cleaved PARP. Phosphorylated PERK was significantly induced by thapsigargin at both 6 and 24 h, while the effects of SW01789 were minimal. Alterations in phosphorylated eIF2α were variable and not significantly different with any treatment at 6 and 24 h. BiP induction by SW016789 was slightly increased at 6 h, although insignificant (P=0.115 vs DMSO 6 h), while thapsigargin induced BiP by 24 h. In agreement with an overall weaker induction of the PERK arm of the UPR^{ER} by SW016789, ATF3 and ATF4 protein expression was induced only at 6 h and to a lesser extent than with thapsigargin (**Fig. 7b**). Amounts of beta cell transcription factors Pdx1 and MafA were unaltered by 6 or 24 h of SW016789 or thapsigargin (**Fig. 7c**). Together, these results partially explain why even though SW016789 amplified secretion and caused ER stress, beta cells only ceased their secretory function and did not undergo terminal UPR^{ER}.

Effects of SW016789 require Ca^{2+} influx

The UPR^{ER} effects of SW016789 in beta cells appeared to stem from the enhancement of nutrient-stimulated Ca^{2+} influx and insulin secretion. To elucidate the mechanisms underlying SW016789-induced hypersecretion of insulin and subsequent UPR^{ER} induction, we took two chemical approaches. First, we co-treated beta cells acutely with SW016789 and candidate compounds to identify any synergy or disruption in SW016789 actions. PKC activation by the phorbol ester phorbol 12-myristate 13-acetate (PMA) is well known to enhance insulin secretion [24, 25]. SW016789 and PMA each independently amplified GSIS (**ESM Fig. 5a**). Unexpectedly, the combination of PMA and SW016789 elicited a marked insulin secretion response in the absence of nutrients. To determine whether PMA-activated PKCs are required for SW016789 action, we pre-treated beta cells overnight with PMA to degrade PKCs [25] and repeated the experiment. Under these conditions, SW016789 and PMA no longer stimulated secretion in the absence of nutrients and the effect of SW016789 on GSIS was no longer significant. These results indicate SW016789 may act in part though PKCs to elicit its acute effects. We also tested the effects of directly opening VDCCs in the presence or absence of SW016789. The potent VDCC activator FPL64176 phenocopied SW016789 in acute and chronic assays in beta cells (**ESM Fig. 5b**). FPL64176 had distinct characteristics, including acutely synergizing with SW016789 in the absence of nutrients to induce Ca^{2+} influx and insulin secretion (**ESM Fig. 5c,d**) and impacting GSCa almost immediately compared to the more delayed effect of SW016789 (**ESM Fig. 5d**). These data suggested that FPL64176 and SW016789 act by different mechanisms.

Second, using a chemical suppressor approach we aimed to disrupt potentially involved pathways by co-treating cells with SW016789 and with compounds having known mechanisms. Compounds were tested for their ability to protect against chronic inhibitory effects of SW016789 (**Fig. 8a, ESM Table 2**) and the VDCC blocker nifedipine was identified as a hit. Co-treatment of InsGLuc-MIN6 beta cells with SW016789 and nifedipine significantly blocked the chronic inhibitory effects of SW016789 on GSIS (**Fig. 8b**) and partially mitigated the induction of *Ddit3* (CHOP) expression at 6 h (**Fig. 8c**). We confirmed the acute potentiating effects of SW016789 on GSIS were indeed dependent on VDCC-mediated Ca^{2+} influx, as co-treatment with nifedipine completely blocked all stimulated secretion in the presence or absence of SW016789 (**Fig. 8d**). The protective effects of nifedipine against SW016789 were confirmed in human islets (**Fig. 8e**), providing additional support that the pathway engaged by SW016789 is conserved between mouse and human beta cells.

DISCUSSION

Role of pharmacological modulation of VDCC activity for beta cell protective effects

Ca^{2+} channel blockers have been in the spotlight for their therapeutic value in both type 1 [26] and type 2 diabetes [27]. For example, verapamil improved beta cell function in a clinical trial of recent-onset type 1 diabetes [26]. The proposed mechanism of action is that suppressing beta cell Ca^{2+} influx reduces expression of the cellular redox regulator *Txnip*, leading to protection from apoptosis [28]. In our studies SW016789 did not induce *Txnip*, suggesting an alternate mechanism. In addition, the VDCC blockers of the dihydropyridine class (nifedipine, nimodipine, amlodipine), as well as the phenylalkylamine class (verapamil) protected beta cells from SW016789-induced dysfunction. Our results showing the protective effects of nifedipine agree with previous findings in beta cells using other stressors including hyperglycaemia and palmitate [29-31]. Distinct VDCC inhibitor mechanisms of action may underlie the differences between dihydropyridine and phenylalkylamine-mediated beta cell protection [32] and may imply that SW016789 acts through a mechanism or pathway which is more dependent on VDCCs in the inactivated state. Because amplified GSCa was confirmed as a major mechanism underlying the effects of SW016789, we hypothesised that directly activating VDCCs using FPL64176 could phenocopy SW016789 [33]. While SW016789 activity on Ca^{2+} influx was inhibited by nifedipine, it also synergized with FPL64176 to enhance Ca^{2+} influx and secretion. The kinetics of Ca^{2+} influx induced by FPL64176 or SW016789 in the presence of glucose differed greatly. In agreement with our findings with FPL64176 and SW016789, prior work showed that chronic treatment with VDCC activator BayK8644 caused insulin secretion defects attributed to decreased abundance of K_{ATP} channel and VDCC subunits [34]. Although not assessed in those studies, beta cells likely underwent transient UPR^{ER} concomitant with or prior to losing function.

Nifedipine or newer generation dihydropyridines like amlodipine, may also be useful therapeutics for conditions that cause hyperinsulinemia or where beta cell VDCCs are dysfunctional. A recent example is an individual with congenital hyperinsulinism with a gain-of-function mutation at a conserved residue in the α1 pore-forming subunit of Cav1.3 (L271H), encoded by *CACNA1D* [35]. Hyperinsulinism in this individual was successfully treated with nifedipine and diazoxide. However, chronic blockade of beta cell VDCCs should be carefully considered, as preliminary findings with genetic deletion of Cav1.3 in mice suggest a positive role in beta cell mass [36]. Auxiliary channel subunits can also impact beta cell function in diabetes. For example, the VDCC β_3 subunit (*Cacnb3*) is upregulated in islets from diabetic animals and was associated with decreased channel function. Deletion of *Cacnb3* improved beta cell function in a mouse model of diabetes [37, 38]. Future research into precision targeting of VDCCs or their regulatory partners may be a promising avenue for diseases of beta cell dysfunction.

Deconvolving the mechanism of action of SW016789

A few conclusions can be made about the mechanism of SW016789 based on the acute phenotype in beta cells. GSCa and GSIS were enhanced by SW016789, but KCl-induced responses were unaffected, suggesting the involvement of metabolism. Metabolic measurements suggested that SW016789 affects nutrient-induced insulin secretion downstream of ATP generation to enhance Ca^{2+} influx. We discovered intersections of SW016789-mediated actions with the PKC activator PMA and VDCC activator FPL64176. This raised concerns about the requirement for nutrient-stimulated ATP production given that SW016789, PMA, and FPL64176 are not nutrients and individually do not stimulate substantial Ca^{2+} influx or insulin secretion (**ESM Fig. 5**). In beta cells, phorbol esters potentiate GSIS through PKC activation [39, 40], but PKCs are not required for normal GSIS [25, 41]. Synergy between phorbol esters and SW016789 may occur through PKC-mediated phosphorylation of substrates involved in insulin exocytosis that lower the threshold for SW016789 to cause enhanced Ca^{2+} influx [42]. We also observed a small, but clear impact of SW016789 on Ca^{2+} influx and InsGLuc secretion in the presence of diazoxide and low KCl which was glucose-dependent (**Fig. 2c, ESM 2c)**. This suggests SW016789 can bypass K_{ATP} to cause membrane depolarization or VDCC opening. Perhaps SW016789 outcompetes the effect of diazoxide on K_{ATP}, although we think this is unlikely because of estimations that >90% of K_{ATP} channels must close before beta cells depolarize [43, 44].

Among compounds tested for protection against SW016789, the most consistent hits were from the dihydropyridine VDCC inhibitor family. We surmise that preventing increased Ca^{2+} influx abrogates SW016789-enhanced insulin secretion, thereby preventing downstream UPR^{ER} and preserving beta cell function. As blocking VDCCs prevents both Ca^{2+} influx and subsequent insulin secretion, it is unclear whether downstream stress and functional loss is induced specifically because of chronically increased Ca^{2+}, enhanced insulin release, or both. Indeed, genetically reducing insulin production by 50% mitigated stress in mouse beta cells [45], suggesting the possibility that in our system, blocking insulin secretion itself using VDCC inhibitors may be responsible for mitigating hypersecretion-induced stress.

Beta cell adaptation and dysfunction in response to chronic secretory demand

Chronic metabolic stress leads to beta cell dysfunction and two recent studies provide prime examples [46, 47]. Sustained physiological hyperglycaemia (72 h) increases absolute insulin secretion but impairs beta cell function as gauged by the disposition index [46]. Accordingly, human islets exposed to glucolipotoxic stress for 48 h were unable to recover GSIS, while islets exposed to milder stress (high glucose or palmitate alone) were able to recover function [47]. Under our culture conditions SW016789 initially potentiated beta cell function, but the secretory response shut down by 4 h. Beta cells recovered from this inhibited state after a 48 h washout, indicating the changes were reversible.

SW016789 selectively and transiently induced canonical UPR^{ER} stress response genes, but with a distinct temporal pattern from that of thapsigargin. Our findings also agree with the apparent lack of oxidative stress induction by SW016789 including no changes in GSH:GSSG or *Txnip*. SW016789-treated beta cells were therefore able to downregulate their response to enhanced Ca^{2+} influx. Relative induction of pro-survival versus pro-apoptotic genes may underlie the effects of SW016789-mediated UPR^{ER}. For example, the Ca^{2+}-activated gene *Npas4* was shown to have a protective role in beta cells and was highly induced by SW016789 [48, 49]. A gene program that mitigates stress within the first 6 h of drug treatment may allow SW016789-treated beta cells to downregulate UPR^{ER} pathway before the point of no return. SW016789 will be a useful tool compound for discovering genes involved in adaptive versus maladaptive responses to chronic Ca^{2+} influx or secretory pressure.

In conclusion, we discovered a new compound and potentially novel pathway that modulates beta cell function and may expand the cohort of targets for disease mitigation. Simultaneously, these discoveries also generate new knowledge about the mechanics of nutrient- and hormone-regulated exocytosis from specialized secretory cell types, including insights into the metabolic amplifying pathway.

FIGURE LEGENDS

Fig. 1. Discovery of SW016789 as a small molecule chronic suppressor of insulin secretion. (a) High-throughput screening workflow leading to the discovery of SW016789. Screening was performed on an 8,320-compound diversity subset approximately representing the chemical space of a >200,000 compound library at the UT Southwestern Medical Center High-Throughput Screening Core. Cells were treated with control and test compounds for 24 h in normal medium followed by a washout and stimulation with glucose and KCl in the presence of diazoxide and finally subjected to InsGLuc assays. These maximal stimulatory conditions afforded the assay a large dynamic range (average Z-score >0.5) and resulted in 168 primary hits which after structural clustering were narrowed down to 82, of which 32 confirmed in triplicate. **(b)** Dose-response testing to determine EC_{50} of SW016789 InsGLuc-MIN6 after a 24 h exposure. Data are the mean ± SD of three independent assays. **(c,d)** In both mouse InsGLuc MIN6 beta cells (**c**) and human islets (**d**), 24 h exposure to SW016789 (5 μM) resulted in suppression of GSIS during assays in the absence of compound. Data are the mean ± SD of 3-4 independent experiments. **(e)** Exposure of MIN6 beta cells to DMSO (0.1%) or SW016789 (5 μM) for up to 72 h did not alter relative amounts of live or dead cells, or the live/dead cell ratio. Digitonin (Dgt) treatment was a positive control for cell death added just prior to the assay. **(f)** InsGLuc-MIN6 cells were exposed to SW016789 (5 μM) for 24-72 h followed by a 1 h washout in glucose-free KRBH. Cells were then stimulated for 1 h with the indicated treatments (0G, glucose-free; 20G, glucose 20 mM; Fsk,

forskolin 10 μM; IBMX 100 μM; PMA, phorbol myristate acetate 100 nM). *, P<0.05 vs respective Basal; †, P<0.05 vs respective DMSO. **(g)** InsGLuc-MIN6 cells were exposed to SW016789 (5 μM) for 24 h followed by a 48 h washout in complete medium. Cells were then assayed for glucose-stimulated InsGLuc secretion. All data are the mean ± SD of at least three independent experiments. *, P<0.05 by two-way ANOVA.

Figure 2. Time-course studies and phenotypic assays reveal SW016789 as an acute potentiator of nutrient-stimulated insulin secretion. (a) InsGLuc-MIN6 cells were treated with SW016789 (5 μM) in a time-course as indicated in the diagram. At the end of the time-course, glucose-stimulated InsGLuc secretion was assayed. Data are the mean ± SD of N=4. **(b)** InsGLuc-MIN6 cells were exposed to SW016789 (5 μM) for 1 h during stimulation with glucose (20 mM), leucine (5 mM), or leucine/glutamine (Leu/Gln; 5mM each) or **(c)** in the presence of diazoxide (250 μM) with or without KCl (35 mM) or glucose (20 mM). Data are the mean ± SD of N=3. *, P<0.05 by two-way ANOVA.

Figure 3. SW016789 treatment modulates nutrient-stimulated Ca^{2+} influx and cAMP generation. (a) MIN6 beta cells pre-treated 24 h with SW016789 (5 μM) or DMSO (0.1%) followed by washout prior to glucose-stimulated Ca^{2+} influx assays and **(b)** area-under-the-curve (AUC) calculation. *, P<0.05 by unpaired Student's t-test. **(c-f)** MIN6 beta cells acutely treated with SW016789 (5 μM) or DMSO (0.1%) followed by **(c)** glucose-, **(d)** leucine/glutamine-, or **(e)** KCl-stimulated Ca^{2+} influx assays and **(f)** associated AUCs. Data are the mean ± SD of three independent experiments. *, P<0.05 by two-way ANOVA. **(g)** MIN6 cells stably expressing the cAMP BRET sensor CAMYEL were preincubated in glucose-free KRBH for 1.5 h prior to treating with coelenterazine-400A for 15 min. Baseline BRET was read for 3 min prior to stimulation as indicated. Cells were stimulated with forskolin (Fsk, 10μM) and IBMX (1μM) as a positive control, SW016789 (10 μM) alone, glucose (20 mM) alone, SW016789 and glucose together, or DMSO (0.1%). **(h)** ΔBRET peak area defined using baseline of 0 and ignoring peaks under 0.5 units high and fewer than 10 adjacent points. Data are the mean ± SD of 2-5 independent experiments as indicated by individual data points on the AUC bar graph. *, P<0.05 by two-way ANOVA.

Figure 4. SW016789 does not impact MIN6 beta cell mitochondrial function or canonical glycolysis and TCA cycle metabolites. (a) Experimental design for targeted metabolomics in MIN6 cells preincubated in glucose-free KRBH for 2 h and then treated with or without glucose (0 vs 20 mM) in the presence of DMSO (0.1%) (DMSO_0G and DMSO_20G) or SW016789 (5 μM) (SW_0G and SW_20G). **(b)** KRBH supernatants were collected for insulin ELISA to verify that SW016789 potentiated insulin secretion under these conditions. **(c)** Metabolomic data are represented as the $\log_2$ fold-change with respect to DMSO_0G of three independent experiments. **(d)** Representative metabolites showing

glucose induced changes in glycolysis (glucose 6-phosphate, fructose-1,6-bisphosphate), TCA cycle (citrate, α-ketoglutarate, and malate), amino acids (cysteine, lysine), adenosine monophosphate, and redox potential (reduced glutathione (GSH) / oxidized glutathione (GSSG)) in MIN6 cells. **(e-g)** MIN6 beta cells were subjected to Seahorse analysis. Cells were preincubated in glucose-free KRBH and **(e)** oxygen consumption rate (OCR), **(f)** extracellular acidification rate (ECAR), and **(g)** calculated Seahorse parameters were measured during stimulation with glucose (20 mM) in the presence or absence of SW016789 (5 μM) or DMSO (0.1%). Subsequently all cells were sequentially stimulated with oligomycin, FCCP, and Antimycin A. Data represent the mean ± SD of three independent experiments.

Figure 5. SW016789 transiently induces the unfolded protein response (UPR^{ER}). (a) MIN6 beta cells were treated with DMSO (0.1%), SW016789 (5 μM), or thapsigargin (Tg, 100 nM) in complete medium for 0-24 has indicated. **(b-d)** Compound additions were staggered to allow simultaneous sample harvesting. Expression of **(b)** immediate early genes and **(c)** adaptive and maladaptive UPR^{ER} genes are shown. **(d)** Expression of *Ins1/2* in the time course and **(e)** insulin content. All data are the mean ± SD of three independent experiments. *, P<0.05 vs DMSO.

Figure 6. SW016789 does not cause maladaptive UPR^{ER} at high concentrations. Relative UPR^{ER} gene expression in MIN6 cells treated for either 6 or 24 h with vehicle (0.1% DMSO) or increasing concentrations of SW016789 (1-20 μM). Thapsigargin (100 nM) was included as a positive control at each time point. Data are the mean ± SD of four independent experiments. *, P<0.05 by two-way ANOVA.

Figure 7. SW016789 and thapsigargin have distinct effects on UPR^{ER}-related proteins. (a) MIN6 beta cells were treated with SW016789 (5 μM) or thapsigargin (Tg, 500 nM) for either 6 or 24 h in complete medium and lysates were immunoblotted. Thapsigargin, but not SW016789, induced pro-apoptotic markers CHOP and cleaved-PARP (cl-PARP). Alterations in UPR^{ER} markers pS51-eIF2α, pT980-PERK, and BiP are shown. **(b)** SW016789 and Tg increased the stress-induced transcription factors ATF4 and ATF3. Data are the mean ± SD of 3 independent experiments. **(c)** Beta cell transcription factors Pdx1 and MafA were not significantly affected by either drug. Data are the mean ± SD of 2-3 independent experiments. In all immunoblots either actin or GAPDH were used as loading controls. *, P<0.05 by two-way ANOVA.

Figure 8. Chemical suppressor screen uncovers VDCC inhibitors as protective agents in chronic SW016789 treatment in MIN6 beta cells and human islets. (a) InsGLuc-MIN6 cells were co-incubated with SW016789 (5 μM), and candidate small molecules as indicated. Following 24 h

incubation, all treatments were removed and glucose-stimulated InsGLuc secretion responses were assessed. **(b)** InsGLuc-MIN6 cells pretreated in complete medium for 24 h with DMSO (0.1%) or SW016789 (5 μM) in the presence or absence of nifedipine (10 μM). After compound washout cells were stimulated with or without glucose (20 mM) for 1 h for InsGLuc assays. Data are the mean ± SD of five independent experiments. **(c)** Cells were treated as in **(b)** and *Ddit3* gene expression was measured. Data are the mean ± SD of four independent experiments. **(d)** InsGLuc-MIN6 cells were acutely incubated with DMSO (0.1%), nifedipine (10μM), SW016789 (5μM), or nifedipine + SW016789 for 1h in the presence or absence of glucose (20mM). Data are the mean ± SD of four independent experiments. **(e)** Human islets were treated 24 h in complete medium with DMSO (0.1%) and SW016789 (5 μM) in the presence or absence of nifedipine (10 μM). Islets were washed and incubated in low glucose (1 mM) KRBH for 1 h, buffer discarded, then incubated 1 h in low (1 mM) or high (16 mM) glucose KRBH for 1 h. Data represent the mean ± SD of insulin measured in supernatant normalized to total insulin content from five different donor islet preparations. *, $P<0.05$ by two-way ANOVA.

Acknowledgements

We thank past and present members of the Cobb lab, Whitehurst lab and D. Rosenbaum at UT Southwestern; D. Eizirik and M. Cnop at Université libre de Bruxelles; and A. Templin at IBRI for helpful discussions. Thanks to C. Cheng in the Whitehurst lab and C. Llamas in the Mishra lab at UT Southwestern for training and advice on Seahorse experiments. Thanks to the L. Zacharias and the DeBerardinis lab at UT Southwestern for advice on metabolomics analyses. Agonist and antagonist functional data on GPCRs for SW016789 were generously provided by B. Roth's group through the National Institute of Mental Health's Psychoactive Drug Screening Program, Contract # HHSN-271-2018-00023-C (NIMH PDSP). MIN6 beta cells were originally generated by J Miyazaki [50] and were kindly shared with us by the late J.C. Hutton. Human QGP1 somatostatinoma cells were a gift from D. Quelle (University of Iowa Carver College of Medicine). Mouse intestinal GLUTag L cells were originally generated by D. Drucker (Mount Sinai Hospital) and were shared with us by the lab of G.G. Holz (Upstate Medical University).

Data availability: All data generated or analyzed during this study are included in this published article (and its electronic supplementary materials).

Funding: This work was supported by the Juvenile Diabetes Research Foundation (2-SRA-2019-702-Q-R to MAK), the Diabetes Research Connection (to MAK), internal funding from the Indiana Biosciences Research Institute (to MAK), and the Welch Foundation (I1243 to MHC). Human

pancreatic islets were provided by the National Institute of Diabetes and Digestive and Kidney Diseases (NIDDK)-funded Integrated Islet Distribution Program (IIDP) (RRID:SCR_014387) at City of Hope (National Institutes of Health Grant # 2UC4DK098085) and the JDRF-funded IIDP Islet Award Initiative (BS438P to MAK).

Authors' relationships and activities: Authors have nothing to disclose.

Contribution statement:

Conceptualization: M.A. Kalwat.

Data curation: M.A. Kalwat.

Formal analysis: K. Rodrigues-dos-Santos, G. Roy, D.D. Binns, F. Armoo, and M.A. Kalwat.

Funding acquisition: M.A. Kalwat and M.H. Cobb.

Investigation: K. Rodrigues-dos-Santos, G. Roy, D.D. Binns, M.G. Grzemska, F. Armoo, M.K. McCoy, A. Huynh, J.Z. Yang, and M.A. Kalwat.

Methodology: M.A. Kalwat.

Project administration: M.A. Kalwat.

Resources: B.A. Posner, M.H. Cobb, and M.A. Kalwat

Supervision: M.H. Cobb and M.A. Kalwat

Validation: K. Rodrigues-dos-Santos, G. Roy, D.D. Binns, M.G. Grzemska, J.Z. Yang, and M.A. Kalwat.

Visualization: K. Rodrigues-dos-Santos, G. Roy, and M.A. Kalwat.

Writing - original draft: M.A. Kalwat.

Writing - review & editing: K. Rodrigues-dos-Santos, G. Roy, D.D. Binns, L. Barella, M.H. Cobb, and M.A. Kalwat

M.A. Kalwat is the guarantor and accepts full responsibility for the work and/or the conduct of the study, had access to the data, and controlled the decision to publish.

References

1. Alejandro EU, Gregg B, Blandino-Rosano M, Cras-Meneur C, Bernal-Mizrachi E. Natural history of beta-cell adaptation and failure in type 2 diabetes. Mol Aspects Med. 2015;42:19-41. doi: 10.1016/j.mam.2014.12.002. PMID: 25542976. PMCID: PMC4404183.

2. Berger C, Zdzieblo D. Glucose transporters in pancreatic islets. Pflugers Arch. 2020;472(9):1249-72. doi: 10.1007/s00424-020-02383-4. PMID: 32394191. PMCID: PMC7462922.

3. Rorsman P, Ashcroft FM. Pancreatic beta-Cell Electrical Activity and Insulin Secretion: Of Mice and Men. Physiol Rev. 2018;98(1):117-214. doi: 10.1152/physrev.00008.2017. PMID: 29212789. PMCID: PMC5866358.

4. Lewandowski SL, Cardone RL, Foster HR, Ho T, Potapenko E, Poudel C, et al. Pyruvate Kinase Controls Signal Strength in the Insulin Secretory Pathway. Cell Metab. 2020;32(5):736-50 e5. doi: 10.1016/j.cmet.2020.10.007. PMID: 33147484. PMCID: PMC7685238.

5. Nicholls DG. The Pancreatic beta-Cell: A Bioenergetic Perspective. Physiol Rev. 2016;96(4):1385-447. doi: 10.1152/physrev.00009.2016. PMID: 27582250.

6. Thurmond DC, Gaisano HY. Recent insights into beta-cell exocytosis in type 2 diabetes. J Mol Biol. 2019. doi: 10.1016/j.jmb.2019.12.012. PMID: 31863749.

7. Henquin JC. Triggering and amplifying pathways of regulation of insulin secretion by glucose. Diabetes. 2000;49(11):1751-60. doi: 10.2337/diabetes.49.11.1751. PMID: 11078440.

8. Kalwat MA, Cobb MH. Mechanisms of the amplifying pathway of insulin secretion in the beta cell. Pharmacol Ther. 2017;179:17-30. doi: 10.1016/j.pharmthera.2017.05.003. PMID: 28527919. PMCID: PMC7269041.

9. Prentki M, Matschinsky FM, Madiraju SR. Metabolic signaling in fuel-induced insulin secretion. Cell Metab. 2013;18(2):162-85. doi: 10.1016/j.cmet.2013.05.018. PMID: 23791483.

10. Kalwat MA, Scheuner D, Rodrigues Dos Santos K, Eizirik DL, Cobb MH. The pancreatic beta cell response to secretory demands and adaption to stress. Endocrinology. 2021. doi: 10.1210/endocr/bqab173. PMID: 34407177.

11. Delepine M, Nicolino M, Barrett T, Golamaully M, Lathrop GM, Julier C. EIF2AK3, encoding translation initiation factor 2-alpha kinase 3, is mutated in patients with Wolcott-Rallison syndrome. Nat Genet. 2000;25(4):406-9. doi: 10.1038/78085. PMID: 10932183.

12. Shalev A, Pise-Masison CA, Radonovich M, Hoffmann SC, Hirshberg B, Brady JN, et al. Oligonucleotide microarray analysis of intact human pancreatic islets: identification of glucose-responsive genes and a highly regulated TGFbeta signaling pathway. Endocrinology. 2002;143(9):3695-8. doi: 10.1210/en.2002-220564. PMID: 12193586.

13. Oyadomari S, Koizumi A, Takeda K, Gotoh T, Akira S, Araki E, et al. Targeted disruption of the Chop gene delays endoplasmic reticulum stress–mediated diabetes. Journal of Clinical Investigation. 2002;109(4):525-32. doi: 10.1172/jci200214550.

14. Sharma RB, O'Donnell AC, Stamateris RE, Ha B, McCloskey KM, Reynolds PR, et al. Insulin demand regulates beta cell number via the unfolded protein response. J Clin Invest. 2015;125(10):3831-46. doi: 10.1172/JCI79264. PMID: 26389675. PMCID: PMC4607122.

15. Lee H, Lee YS, Harenda Q, Pietrzak S, Oktay HZ, Schreiber S, et al. Beta Cell Dedifferentiation Induced by IRE1alpha Deletion Prevents Type 1 Diabetes. Cell Metab. 2020;31(4):822-36 e5. doi: 10.1016/j.cmet.2020.03.002. PMID: 32220307. PMCID: PMC7346095.

16. Eizirik DL, Pasquali L, Cnop M. Pancreatic beta-cells in type 1 and type 2 diabetes mellitus: different pathways to failure. Nat Rev Endocrinol. 2020;16(7):349-62. doi: 10.1038/s41574-020-0355-7. PMID: 32398822.

17. Engin F. ER stress and development of type 1 diabetes. J Investig Med. 2016;64(1):2-6. doi: 10.1097/JIM.0000000000000229. PMID: 26230493.

18. Herbert TP, Laybutt DR. A Reevaluation of the Role of the Unfolded Protein Response in Islet Dysfunction: Maladaptation or a Failure to Adapt? Diabetes. 2016;65(6):1472-80. doi: 10.2337/db15-1633. PMID: 27222391.

19. Burns SM, Vetere A, Walpita D, Dancik V, Khodier C, Perez J, et al. High-throughput luminescent reporter of insulin secretion for discovering regulators of pancreatic Beta-cell function. Cell Metab. 2015;21(1):126-37. doi: 10.1016/j.cmet.2014.12.010. PMID: 25565210.

20. Kalwat MA, Wichaidit C, Nava Garcia AY, McCoy MK, McGlynn K, Hwang IH, et al. Insulin promoter-driven Gaussia luciferase-based insulin secretion biosensor assay for discovery of beta-cell glucose-sensing pathways. ACS Sens. 2016;1(10):1208-12. doi: 10.1021/acssensors.6b00433. PMID: 27819058. PMCID: PMC5089812.

21. Kalwat MA. High-Throughput Screening for Insulin Secretion Modulators. Methods Mol Biol. 2021;2233:C1. doi: 10.1007/978-1-0716-1044-2_22. PMID: 33502748.

22. Jiang LI, Collins J, Davis R, Lin KM, DeCamp D, Roach T, et al. Use of a cAMP BRET sensor to characterize a novel regulation of cAMP by the sphingosine 1-phosphate/G13 pathway. J Biol Chem. 2007;282(14):10576-84. doi: 10.1074/jbc.M609695200. PMID: 17283075. PMCID: PMC2526465.

23. Kroeze WK, Sassano MF, Huang XP, Lansu K, McCorvy JD, Giguere PM, et al. PRESTO-Tango as an open-source resource for interrogation of the druggable human GPCRome. Nat Struct Mol Biol. 2015;22(5):362-9. doi: 10.1038/nsmb.3014. PMID: 25895059. PMCID: PMC4424118.

24. Santo-Domingo J, Chareyron I, Dayon L, Nunez Galindo A, Cominetti O, Pilar Giner Gimenez M, et al. Coordinated activation of mitochondrial respiration and exocytosis mediated by PKC signaling in pancreatic beta-cells. FASEB J. 2016. doi: 10.1096/fj.201600837R. PMID: 27927723.

25. Yaney GC, Fairbanks JM, Deeney JT, Korchak HM, Tornheim K, Corkey BE. Potentiation of insulin secretion by phorbol esters is mediated by PKC-alpha and nPKC isoforms. Am J Physiol Endocrinol Metab. 2002;283(5):E880-8. doi: 10.1152/ajpendo.00474.2001. PMID: 12376314.

26. Ovalle F, Grimes T, Xu G, Patel AJ, Grayson TB, Thielen LA, et al. Verapamil and beta cell function in adults with recent-onset type 1 diabetes. Nat Med. 2018;24(8):1108-12. doi: 10.1038/s41591-018-0089-4. PMID: 29988125. PMCID: PMC6092963.

27. Zhao D, Cao Y, Yu CG, Yuan SS, Zhang N, Zhang YY, et al. The association of calcium channel blockers with beta-cell function in type 2 diabetic patients: A cross-sectional study. J Clin Hypertens (Greenwich). 2019. doi: 10.1111/jch.13517. PMID: 30900372.

28. Xu G, Chen J, Jing G, Shalev A. Preventing beta-cell loss and diabetes with calcium channel blockers. Diabetes. 2012;61(4):848-56. doi: 10.2337/db11-0955. PMID: 22442301. PMCID: PMC3314354.

29. Syeda K, Mohammed AM, Arora DK, Kowluru A. Glucotoxic conditions induce endoplasmic reticulum stress to cause caspase 3 mediated lamin B degradation in pancreatic beta-cells:

protection by nifedipine. Biochem Pharmacol. 2013;86(9):1338-46. doi: 10.1016/j.bcp.2013.08.023. PMID: 23994168. PMCID: PMC3832847.

30. Jeffrey KD, Alejandro EU, Luciani DS, Kalynyak TB, Hu X, Li H, et al. Carboxypeptidase E mediates palmitate-induced beta-cell ER stress and apoptosis. Proceedings of the National Academy of Sciences of the United States of America. 2008;105(24):8452-7. doi: 10.1073/pnas.0711232105. PMID: 18550819. PMCID: PMC2448857.

31. Wang Y, Gao L, Li Y, Chen H, Sun Z. Nifedipine protects INS-1 beta-cell from high glucose-induced ER stress and apoptosis. Int J Mol Sci. 2011;12(11):7569-80. doi: 10.3390/ijms12117569. PMID: 22174617. PMCID: PMC3233423.

32. Tang L, Gamal El-Din TM, Swanson TM, Pryde DC, Scheuer T, Zheng N, et al. Structural basis for inhibition of a voltage-gated Ca(2+) channel by Ca(2+) antagonist drugs. Nature. 2016;537(7618):117-21. doi: 10.1038/nature19102. PMID: 27556947. PMCID: PMC5161592.

33. Zheng W, Rampe D, Triggle D. Pharmacological, radioligand binding, and electrophysiological characteristics of FPL 64176, a novel nondihydropyridine Ca2+ channel activator, in cardiac and vascular preparations. Mol Pharm. 1991;40(5):734-41. PMCID: 1719369.

34. Minami K, Yokokura M, Ishizuka N, Seino S. Normalization of intracellular Ca(2+) induces a glucose-responsive state in glucose-unresponsive beta-cells. J Biol Chem. 2002;277(28):25277-82. doi: 10.1074/jbc.M203988200. PMID: 12101221.

35. De Mingo Alemany MC, Mifsud Grau L, Moreno Macian F, Ferrer Lorente B, Leon Carinena S. A de novo CACNA1D missense mutation in a patient with congenital hyperinsulinism, primary hyperaldosteronism and hypotonia. Channels (Austin). 2020;14(1):175-80. doi: 10.1080/19336950.2020.1761171. PMID: 32336187.

36. Theiner T, Jacobo-Piqueras N, Ortner NJ, Geisler SM, Tuluc P. CaV1.3 L-type Ca2+ channel modulates pancreatic beta-cell electrical activity and survival. J Gen Physiol. 2022;154(9). doi: 10.1085/jgp.2021ecc34. PMID: 34767006.

37. Lee K, Kim J, Kohler M, Yu J, Shi Y, Yang SN, et al. Blocking Ca(2+) Channel beta3 Subunit Reverses Diabetes. Cell Rep. 2018;24(4):922-34. doi: 10.1016/j.celrep.2018.06.086. PMID: 30044988. PMCID: PMC6083041.

38. Berggren PO, Yang SN, Murakami M, Efanov AM, Uhles S, Kohler M, et al. Removal of Ca2+ channel beta3 subunit enhances Ca2+ oscillation frequency and insulin exocytosis. Cell. 2004;119(2):273-84. doi: 10.1016/j.cell.2004.09.033. PMID: 15479643.

39. Newton AC. Protein kinase C: perfectly balanced. Crit Rev Biochem Mol Biol. 2018;53(2):208-30. doi: 10.1080/10409238.2018.1442408. PMID: 29513138. PMCID: PMC5901981.

40. Hii CS, Jones PM, Persaud SJ, Howell SL. A re-assessment of the role of protein kinase C in glucose-stimulated insulin secretion. Biochem J. 1987;246(2):489-93. doi: 10.1042/bj2460489. PMID: 3318809. PMCID: PMC1148300.

41. Jones PM, Persaud SJ, Howell SL. Insulin secretion and protein phosphorylation in PKC-depleted islets of langerhans. Life Sciences. 1992;50(11):761-7. doi: 10.1016/0024-3205(92)90180-w.

42. Uchida T, Iwashita N, Ohara-Imaizumi M, Ogihara T, Nagai S, Choi JB, et al. Protein kinase Cdelta plays a non-redundant role in insulin secretion in pancreatic beta cells. J Biol Chem. 2007;282(4):2707-16. doi: 10.1074/jbc.M610482200. PMID: 17135234.

43. Thompson B, Satin LS. Beta-Cell Ion Channels and Their Role in Regulating Insulin Secretion. Compr Physiol. 2021;11(4):1-21. doi: 10.1002/cphy.c210004. PMID: 34636409.

44. Cook DL, Satin LS, Ashford ML, Hales CN. ATP-sensitive K+ channels in pancreatic beta-cells. Spare-channel hypothesis. Diabetes. 1988;37(5):495-8. doi: 10.2337/diab.37.5.495. PMID: 2452107.

45. Szabat M, Page MM, Panzhinskiy E, Skovso S, Mojibian M, Fernandez-Tajes J, et al. Reduced Insulin Production Relieves Endoplasmic Reticulum Stress and Induces beta Cell Proliferation. Cell Metab. 2016;23(1):179-93. doi: 10.1016/j.cmet.2015.10.016. PMID: 26626461.

46. Merovci A, Tripathy D, Chen X, Valdez I, Abdul-Ghani M, Solis-Herrera C, et al. Effect of Mild Physiologic Hyperglycemia on Insulin Secretion, Insulin Clearance, and Insulin Sensitivity in Healthy Glucose-Tolerant Subjects. Diabetes. 2021;70(1):204-13. doi: 10.2337/db20-0039. PMID: 33033064. PMCID: PMC7881846.

47. Marselli L, Piron A, Suleiman M, Colli ML, Yi X, Khamis A, et al. Persistent or Transient Human beta Cell Dysfunction Induced by Metabolic Stress: Specific Signatures and Shared Gene Expression with Type 2 Diabetes. Cell Rep. 2020;33(9):108466. doi: 10.1016/j.celrep.2020.108466. PMID: 33264613.

48. Speckmann T, Sabatini PV, Nian C, Smith RG, Lynn FC. Npas4 Transcription Factor Expression Is Regulated by Calcium Signaling Pathways and Prevents Tacrolimus-induced Cytotoxicity in Pancreatic Beta Cells. J Biol Chem. 2016;291(6):2682-95. doi: 10.1074/jbc.M115.704098. PMID: 26663079. PMCID: PMC4742737.

49. Sabatini PV, Krentz NA, Zarrouki B, Westwell-Roper CY, Nian C, Uy RA, et al. Npas4 is a novel activity-regulated cytoprotective factor in pancreatic beta-cells. Diabetes. 2013;62(8):2808-20. doi: 10.2337/db12-1527. PMID: 23656887. PMCID: 3717850.

50. Miyazaki J, Araki K, Yamato E, Ikegami H, Asano T, Shibasaki Y, et al. Establishment of a pancreatic beta cell line that retains glucose-inducible insulin secretion: special reference to expression of glucose transporter isoforms. Endocrinology. 1990;127(1):126-32. doi: 10.1210/endo-127-1-126. PMID: 2163307.

Fig .1

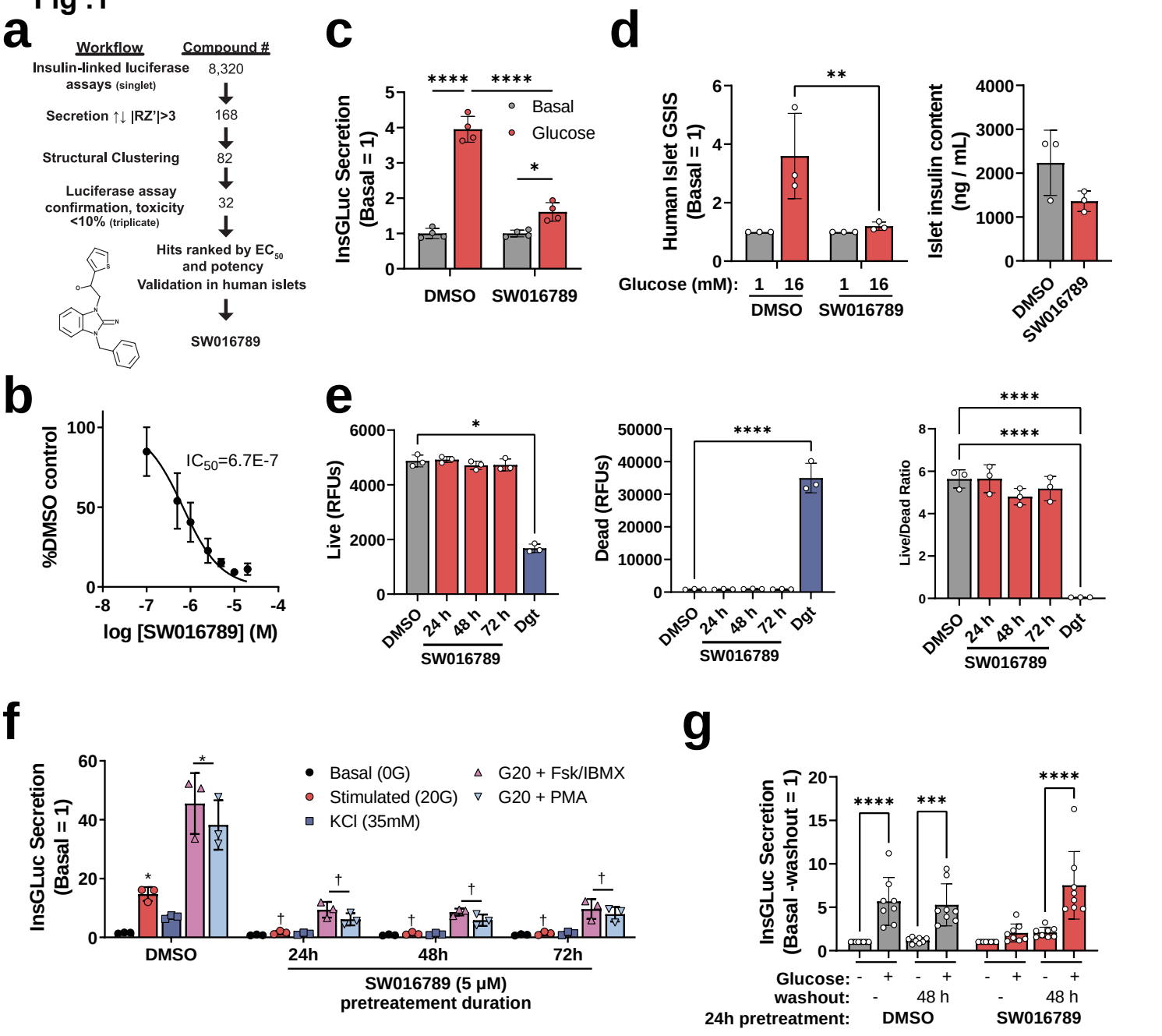
a
Workflow
Compound #
Insulin-linked luciferase assays (singlet)
8,320
Secretion ↑↓ |RZ'|>3
168
Structural Clustering
82
Luciferase assay confirmation, toxicity <10% (triplicate)
32
Hits ranked by EC50 and potency
Validation in human islets
SW016789
b
%DMSO control
IC50=6.7E-7
log [SW016789] (M)
c
InsGLuc Secretion (Basal = 1)
Basal
Glucose
DMSO
SW016789
d
Human Islet GSIS (Basal = 1)
Glucose (mM):
Islet insulin content (ng / mL)
e
Live (RFUs)
Dead (RFUs)
Live/Dead Ratio
DMSO
24 h
48 h
72 h
Dgt
SW016789
f
InsGLuc Secretion (Basal = 1)
Basal (0G)
Stimulated (20G)
KCl (35mM)
G20 + Fsk/IBMX
G20 + PMA
DMSO
24h
48h
72h
SW016789 (5 μM) pretreatement duration
g
InsGLuc Secretion (Basal -washout = 1)
Glucose:
washout:
24h pretreatment:
DMSO
SW016789

Fig . 2

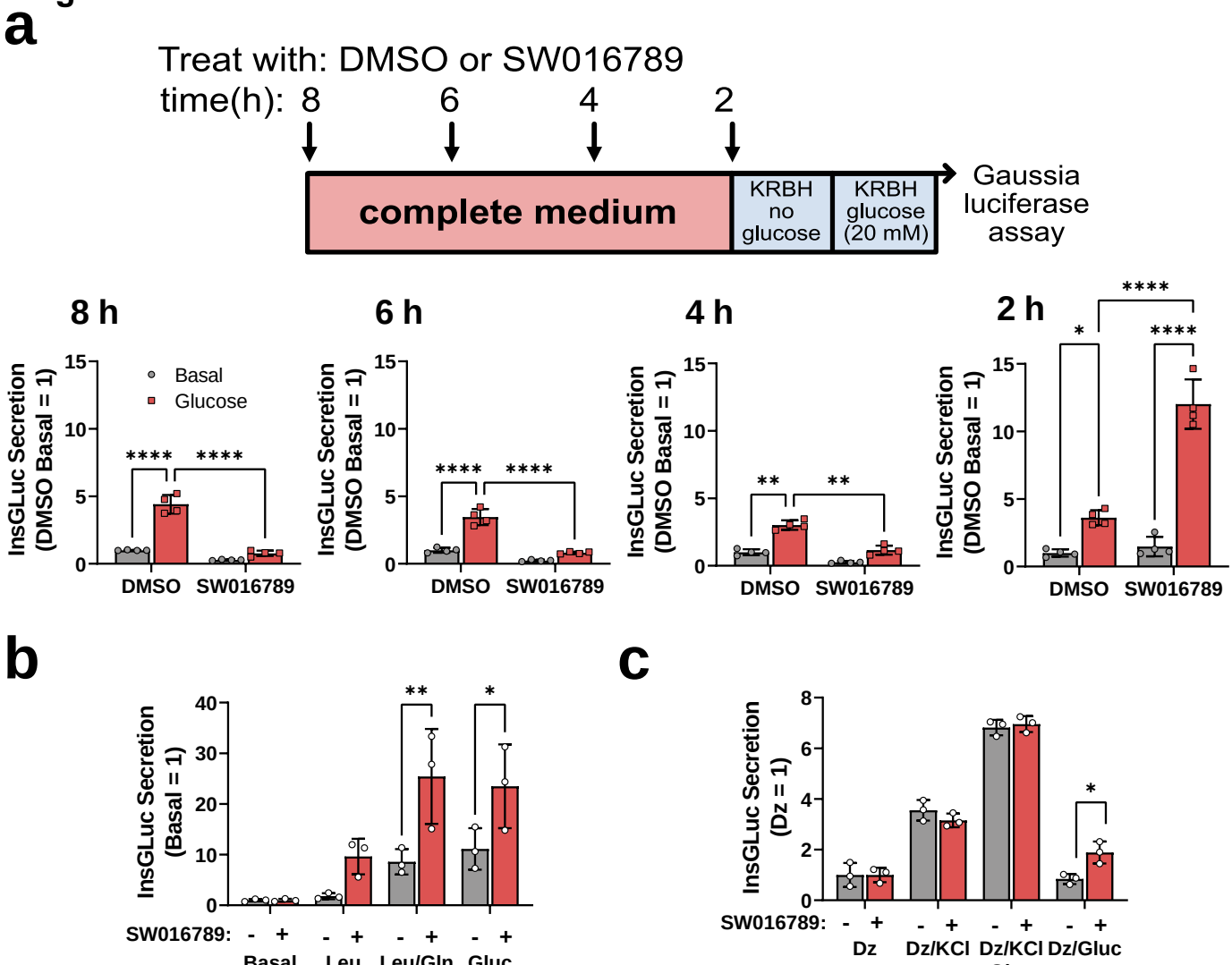
a
Treat with: DMSO or SW016789
time(h): 8 6 4 2
complete medium
KRBH no glucose
KRBH glucose (20 mM)
Gaussia luciferase assay
8 h
6 h
4 h
2 h
Basal
Glucose
InsGLuc Secretion (DMSO Basal = 1)
DMSO
SW016789
b
InsGLuc Secretion (Basal = 1)
SW016789:
Basal
Leu
Leu/Gln
Gluc
c
InsGLuc Secretion (Dz = 1)
Dz
Dz/KCl
Dz/KCl Gluc
Dz/Gluc

Fig. 3

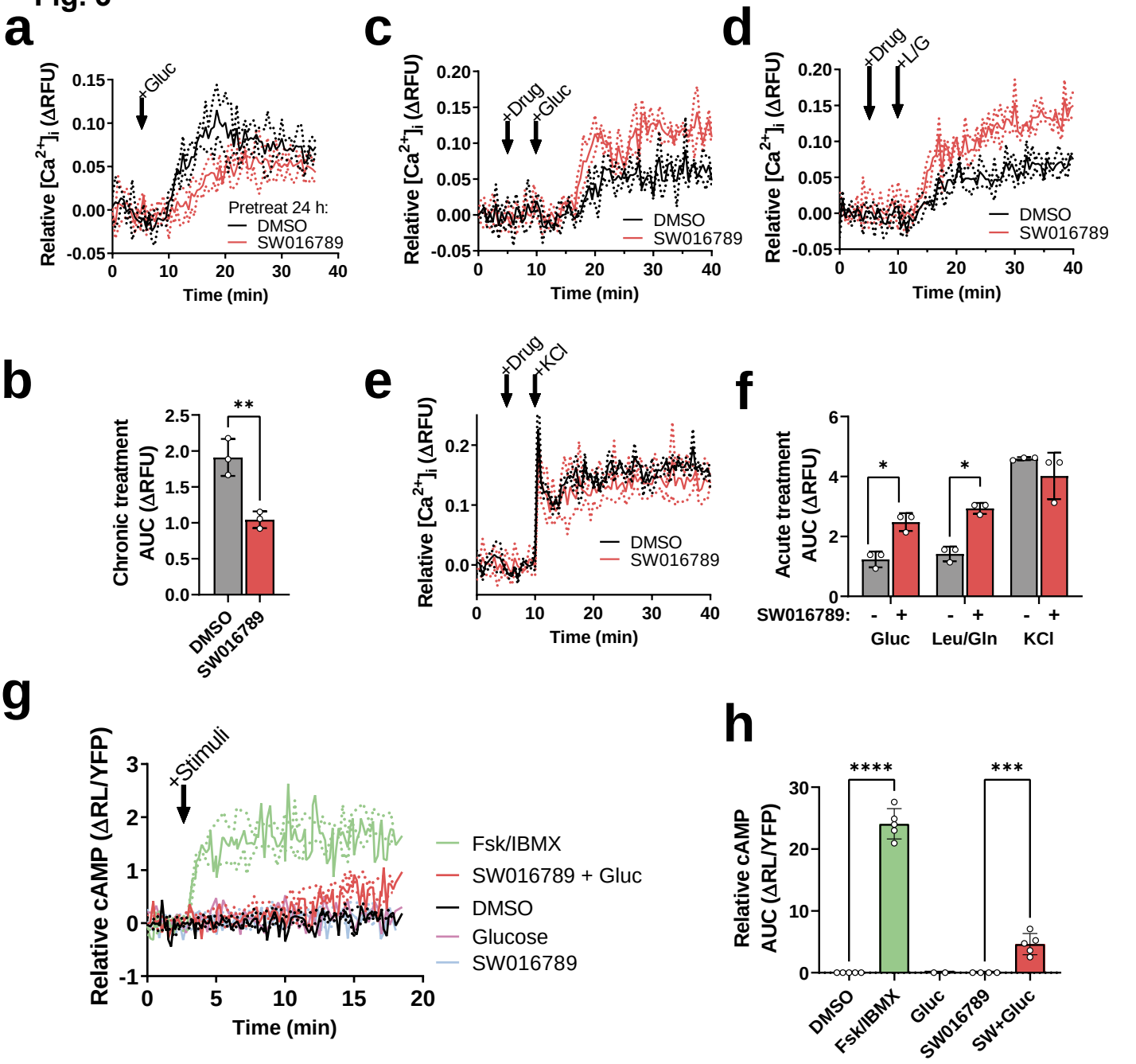
a
+Gluc
Relative [Ca2+]i (ΔRFU)
Pretreat 24 h:
DMSO
SW016789
Time (min)
b
Chronic treatment AUC (ΔRFU)
**
DMSO
SW016789
c
+Drug
+Gluc
DMSO
SW016789
Time (min)
d
+Drug
+L/G
DMSO
SW016789
Time (min)
e
+Drug
+KCl
DMSO
SW016789
Time (min)
f
Acute treatment AUC (ΔRFU)
*
*
SW016789: - + - + - +
Gluc
Leu/Gln
KCl
g
+Stimuli
Relative cAMP (ΔRL/YFP)
Fsk/IBMX
SW016789 + Gluc
DMSO
Glucose
SW016789
Time (min)
h
Relative cAMP AUC (ΔRL/YFP)
****
***
DMSO
Fsk/IBMX
Gluc
SW016789
SW+Gluc

Fig. 4

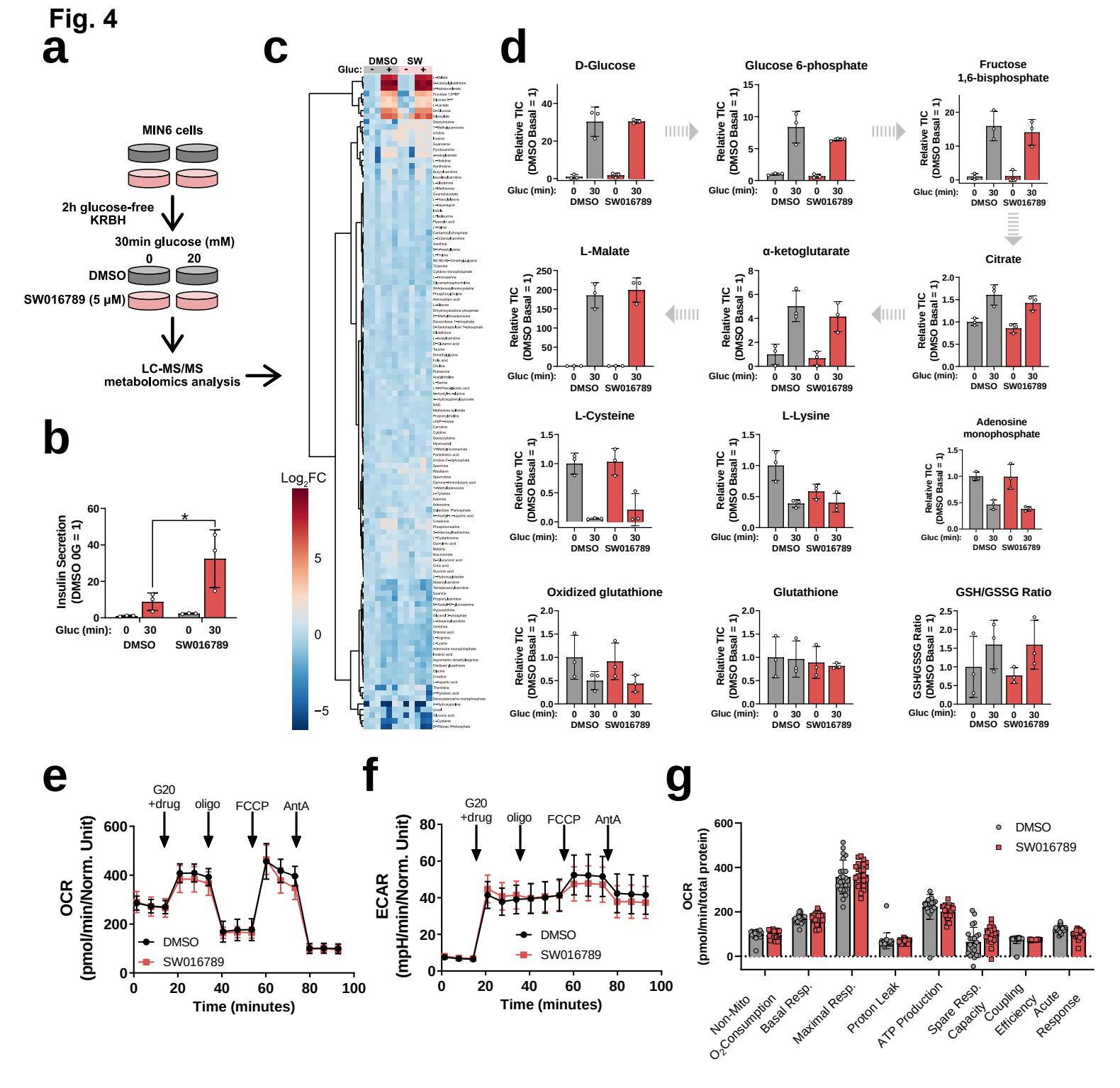
a
MIN6 cells
2h glucose-free KRBH
30min glucose (mM)
0
20
DMSO
SW016789 (5 μM)
LC-MS/MS metabolomics analysis
b
Insulin Secretion (DMSO 0G = 1)
Gluc (min):
DMSO
SW016789
c
Gluc:
DMSO
SW
Log2FC
d
D-Glucose
Glucose 6-phosphate
Fructose 1,6-bisphosphate
L-Malate
α-ketoglutarate
Citrate
L-Cysteine
L-Lysine
Adenosine monophosphate
Oxidized glutathione
Glutathione
GSH/GSSG Ratio
Relative TIC (DMSO Basal = 1)
e
G20 +drug
oligo
FCCP
AntA
OCR (pmol/min/Norm. Unit)
DMSO
SW016789
Time (minutes)
f
ECAR (mpH/min/Norm. Unit)
g
OCR (pmol/min/total protein)
Non-Mito O2 Consumption
Basal Resp.
Maximal Resp.
Proton Leak
ATP Production
Spare Resp. Capacity
Coupling Efficiency
Acute Response

Fig. 5

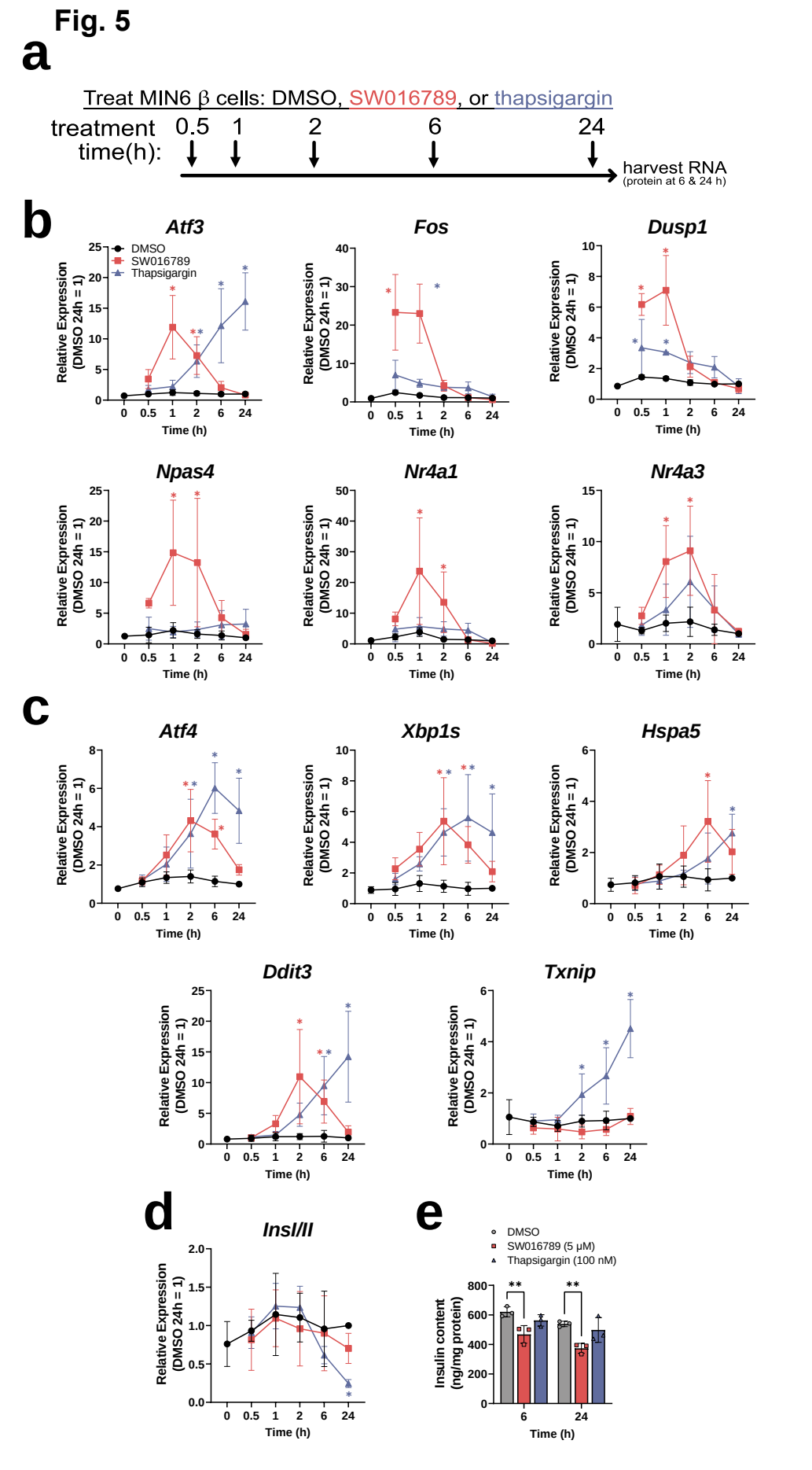
a
Treat MIN6 β cells: DMSO, SW016789, or thapsigargin
treatment time(h): 0.5 1 2 6 24
harvest RNA
(protein at 6 & 24 h)
b
Atf3
Fos
Dusp1
Npas4
Nr4a1
Nr4a3
DMSO
SW016789
Thapsigargin
Relative Expression (DMSO 24h = 1)
Time (h)
c
Atf4
Xbp1s
Hspa5
Ddit3
Txnip
d
Insl/II
e
DMSO
SW016789 (5 μM)
Thapsigargin (100 nM)
Insulin content (ng/mg protein)
Time (h)

Fig. 6

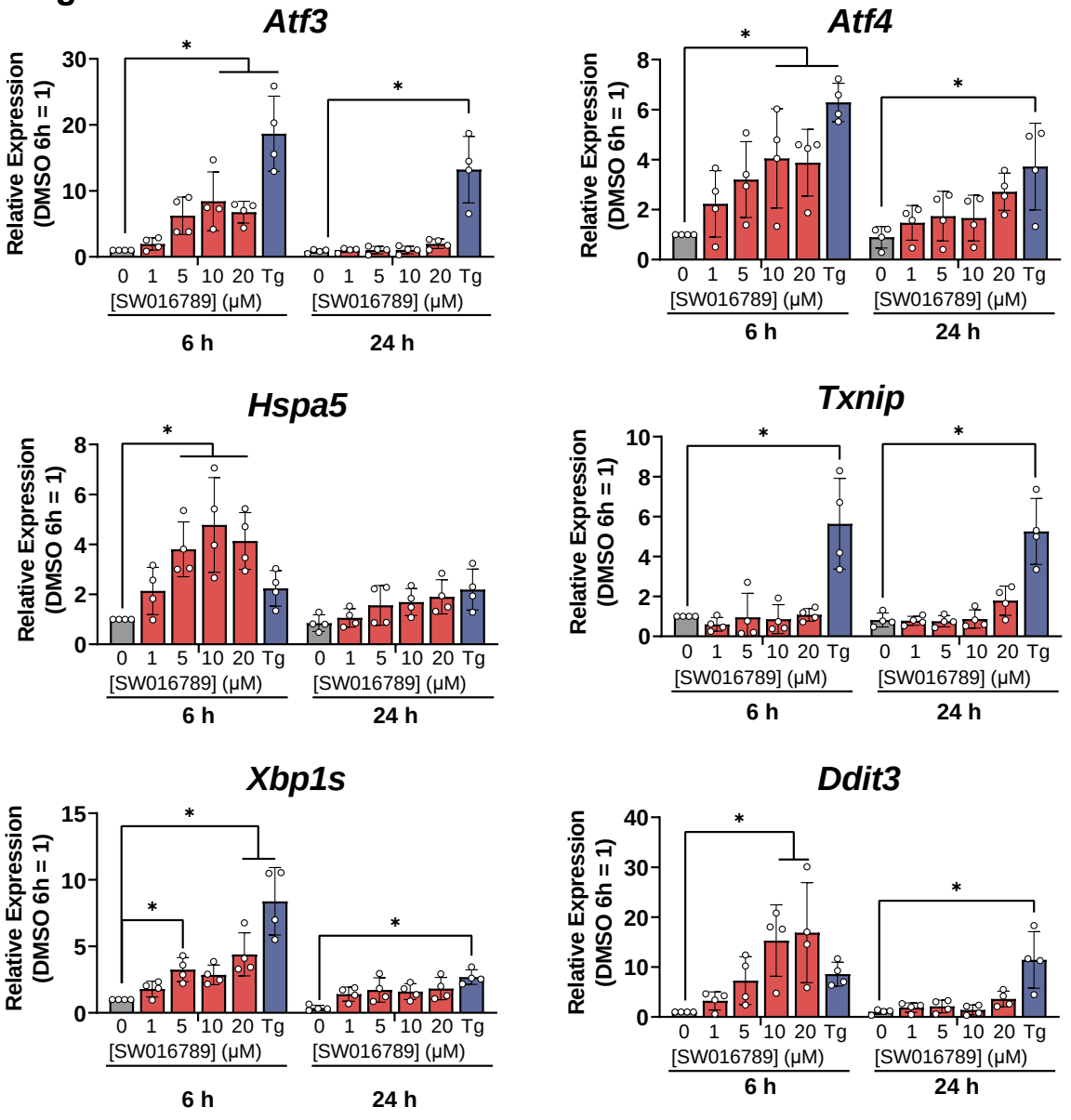
Atf3
Atf4
Hspa5
Txnip
Xbp1s
Ddit3
Relative Expression (DMSO 6h = 1)
0 1 5 10 20 Tg
[SW016789] (μM)
6 h
24 h
*

Fig. 7

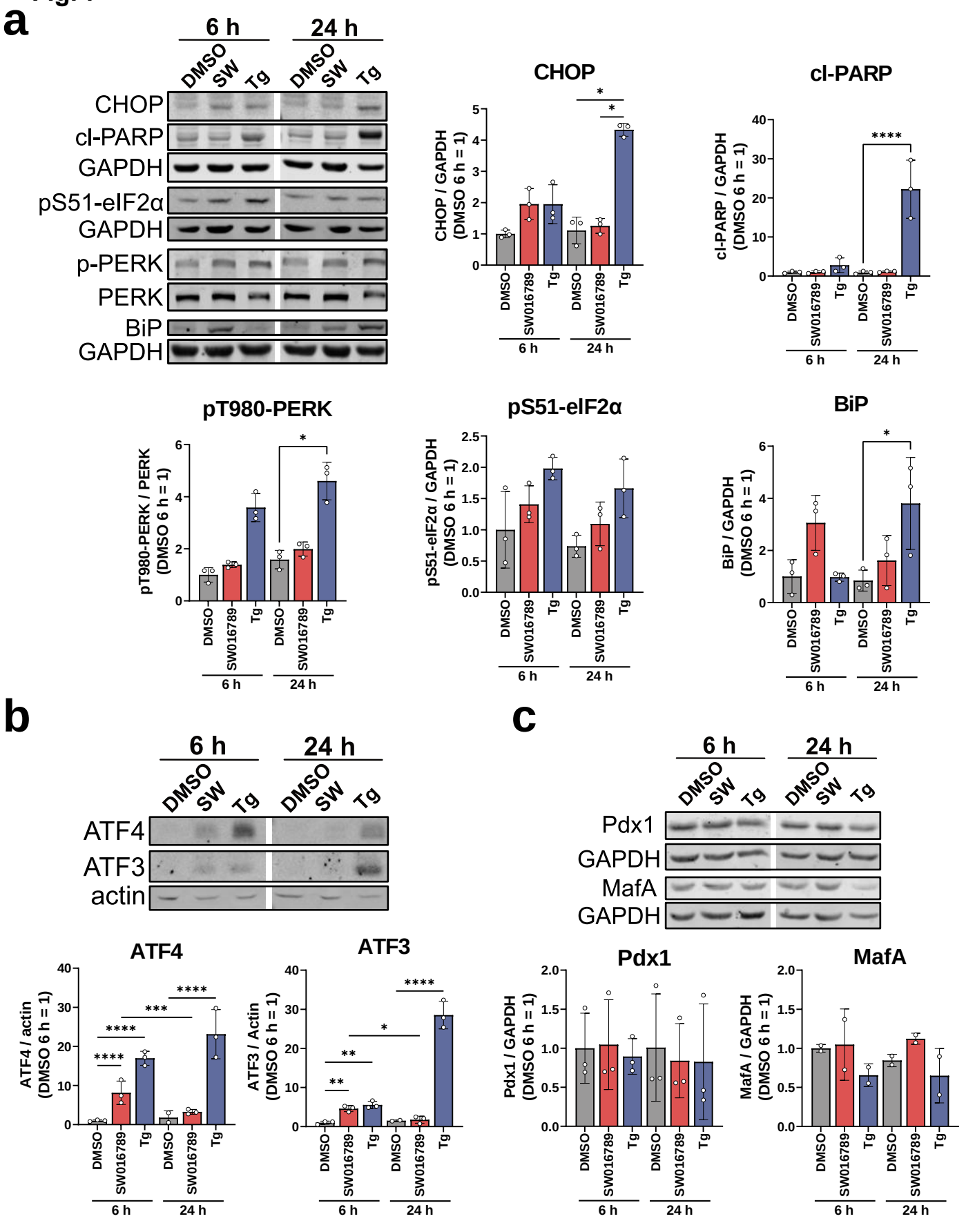
a
6 h
24 h
DMSO
SW
Tg
CHOP
cl-PARP
GAPDH
pS51-eIF2α
GAPDH
p-PERK
PERK
BiP
GAPDH
CHOP
CHOP / GAPDH (DMSO 6 h = 1)
cl-PARP
cl-PARP / GAPDH (DMSO 6 h = 1)
pT980-PERK
pT980-PERK / PERK (DMSO 6 h = 1)
pS51-eIF2α
pS51-eIF2α / GAPDH (DMSO 6 h = 1)
BiP
BiP / GAPDH (DMSO 6 h = 1)
DMSO
SW016789
Tg
6 h
24 h
b
ATF4
ATF3
actin
ATF4
ATF4 / actin (DMSO 6 h = 1)
ATF3
ATF3 / Actin (DMSO 6 h = 1)
c
Pdx1
GAPDH
MafA
GAPDH
Pdx1
Pdx1 / GAPDH (DMSO 6 h = 1)
MafA
MafA / GAPDH (DMSO 6 h = 1)

Fig. 8

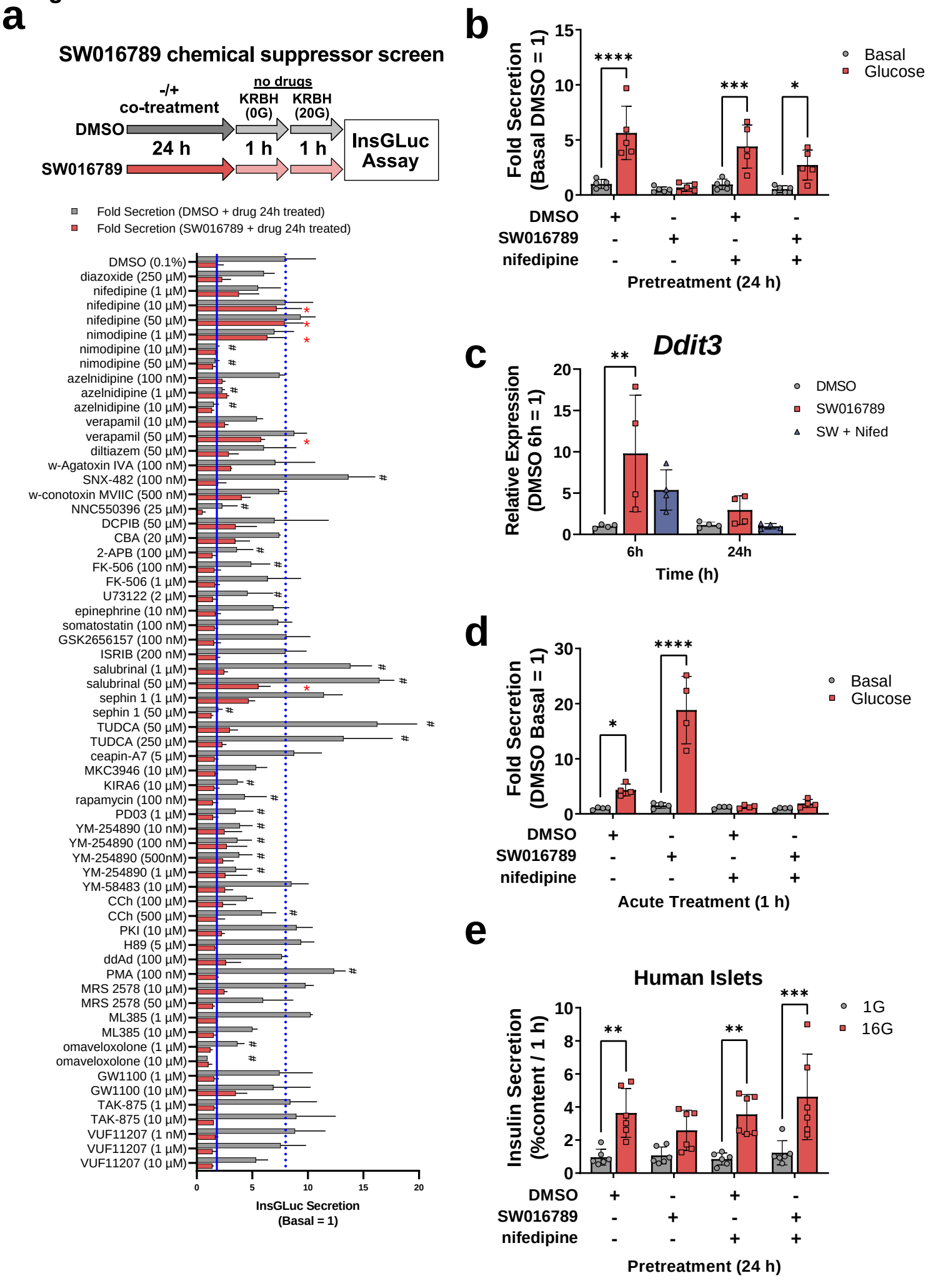
a
SW016789 chemical suppressor screen
-/+ co-treatment
no drugs
KRBH (0G)
KRBH (20G)
DMSO
SW016789
24 h
1 h
1 h
InsGLuc Assay
Fold Secretion (DMSO + drug 24h treated)
Fold Secretion (SW016789 + drug 24h treated)
DMSO (0.1%)
diazoxide (250 μM)
nifedipine (1 μM)
nifedipine (10 μM)
nifedipine (50 μM)
nimodipine (1 μM)
nimodipine (10 μM)
nimodipine (50 μM)
azelnidipine (100 nM)
azelnidipine (1 μM)
azelnidipine (10 μM)
verapamil (10 μM)
verapamil (50 μM)
diltiazem (50 μM)
w-Agatoxin IVA (100 nM)
SNX-482 (100 nM)
w-conotoxin MVIIC (500 nM)
NNC550396 (25 μM)
DCPIB (50 μM)
CBA (20 μM)
2-APB (100 μM)
FK-506 (100 nM)
FK-506 (1 μM)
U73122 (2 μM)
epinephrine (10 nM)
somatostatin (100 nM)
GSK2656157 (100 nM)
ISRIB (200 nM)
salubrinal (1 μM)
salubrinal (50 μM)
sephin 1 (1 μM)
sephin 1 (50 μM)
TUDCA (50 μM)
TUDCA (250 μM)
ceapin-A7 (5 μM)
MKC3946 (10 μM)
KIRA6 (10 μM)
rapamycin (100 nM)
PD03 (1 μM)
YM-254890 (10 nM)
YM-254890 (100 nM)
YM-254890 (500nM)
YM-254890 (1 μM)
YM-58483 (10 μM)
CCh (100 μM)
CCh (500 μM)
PKI (10 μM)
H89 (5 μM)
ddAd (100 μM)
PMA (100 nM)
MRS 2578 (10 μM)
MRS 2578 (50 μM)
ML385 (1 μM)
ML385 (10 μM)
omaveloxolone (1 μM)
omaveloxolone (10 μM)
GW1100 (1 μM)
GW1100 (10 μM)
TAK-875 (1 μM)
TAK-875 (10 μM)
VUF11207 (1 nM)
VUF11207 (1 μM)
VUF11207 (10 μM)
0
5
10
15
20
InsGLuc Secretion (Basal = 1)
b
Fold Secretion (Basal DMSO = 1)
****
***
*
Basal
Glucose
DMSO + - + -
SW016789 - + - +
nifedipine - - + +
Pretreatment (24 h)
c
Ddit3
Relative Expression (DMSO 6h = 1)
**
DMSO
SW016789
SW + Nifed
6h
24h
Time (h)
d
Fold Secretion (DMSO Basal = 1)
*
****
Basal
Glucose
DMSO + - + -
SW016789 - + - +
nifedipine - - + +
Acute Treatment (1 h)
e
Human Islets
Insulin Secretion (%content / 1 h)
**
**
***
1G
16G
DMSO + - + -
SW016789 - + - +
nifedipine - - + +
Pretreatment (24 h)